Supporting Information

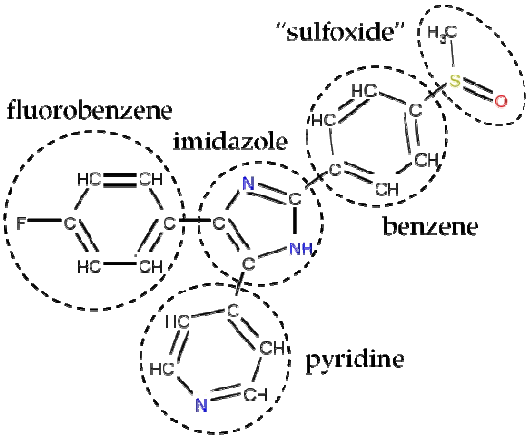

Figure S1. Principal moieties of the inhibitor SB203580. Each of the principal functional groups present in the inhibitor is labeled by a dashed circle. The carbon (and hydrogen), nitrogen, sulfur, and oxygen atoms are colored black, blue, yellow, and red, respectively.

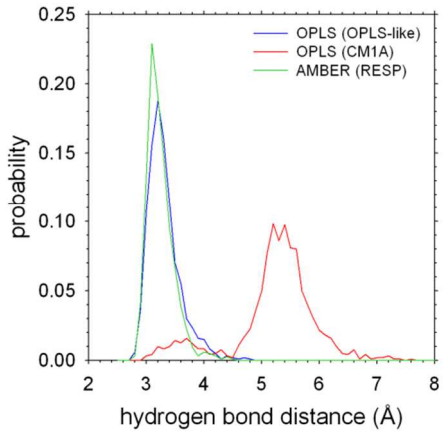

Figure S2. Probability distribution function of the key hydrogen bond observed in simulations of the wild-type p38α-SB203580 complex. Simulations of the wild-type p38α kinase in complex with SB203580 were performed for 12 ns with three different force fields: (a) OPLS-AA/L using partial charges for SB203580 derived by analogy (OPLS-like), (b) OPLS-AA/L using partial charges for SB203580 derived using the CM1A method (CM1A), and (c) Amber ff99SB-ILDN using partial charges for SB203580 derived using the conventional Amber methodology (RESP). In all cases, the hydrogen bond distance is defined in terms of its heavy atoms – i.e. the distance between the N of SB203580's pyridine ring and the backbone N of Met 109 in p38α.

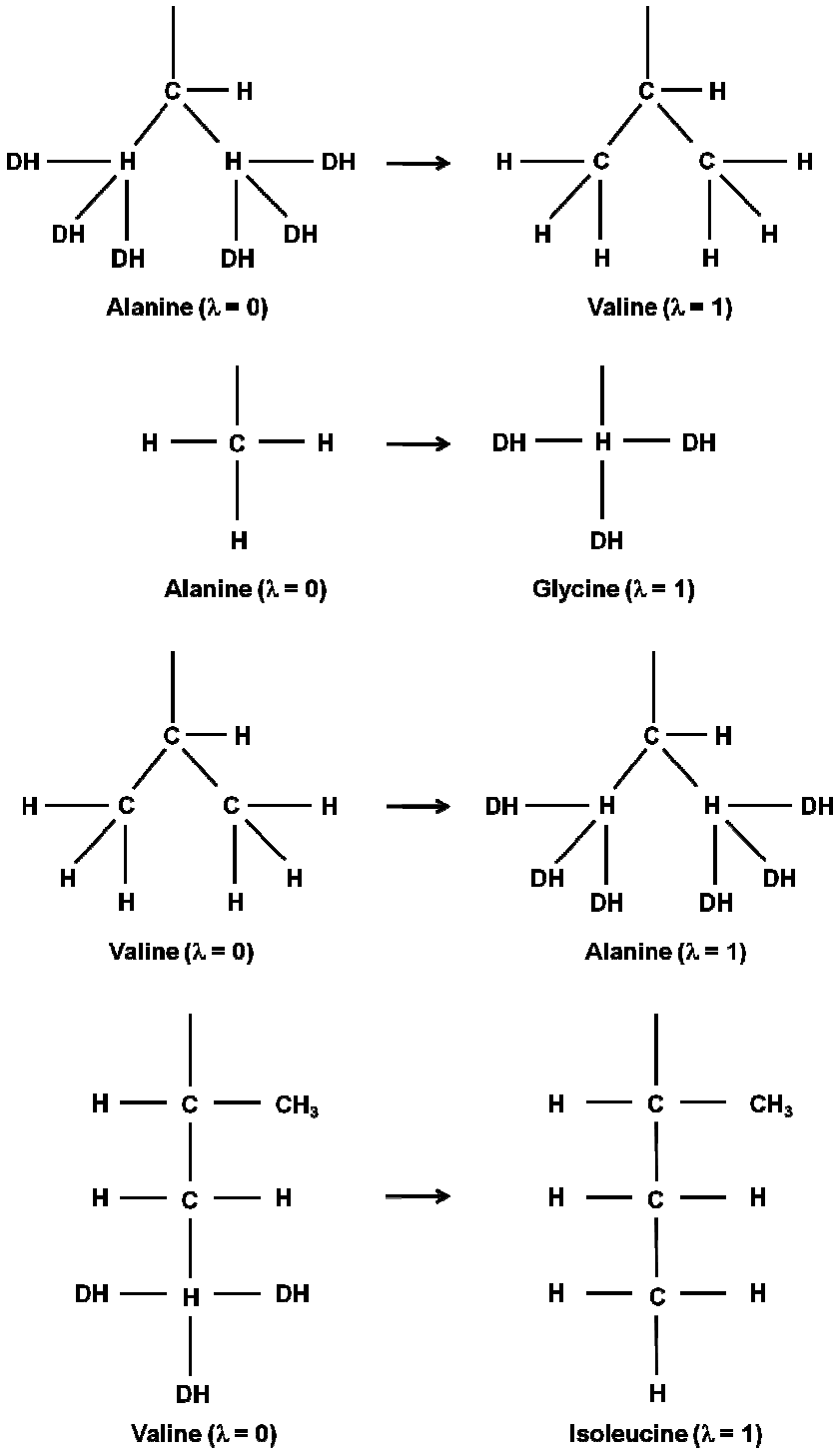

Figure S3. Scheme for performing alchemical transformations of p38α mutants. Shown above from top to bottom are the transformations for four mutations: A51V, A51G, V38A, and V38I. "DH" denotes dummy hydrogen atoms. Only sidechain atoms are shown.

Figure S4. Quadratic fits of the normalized fluorescence data obtained from titrations of p38α protein with SB203580. Each row represents the results of three independent experiments. Solid dots represent experimentally measured data while curves represent fits to the quadratic function. The R^2 and K_d are included on top of each panel.

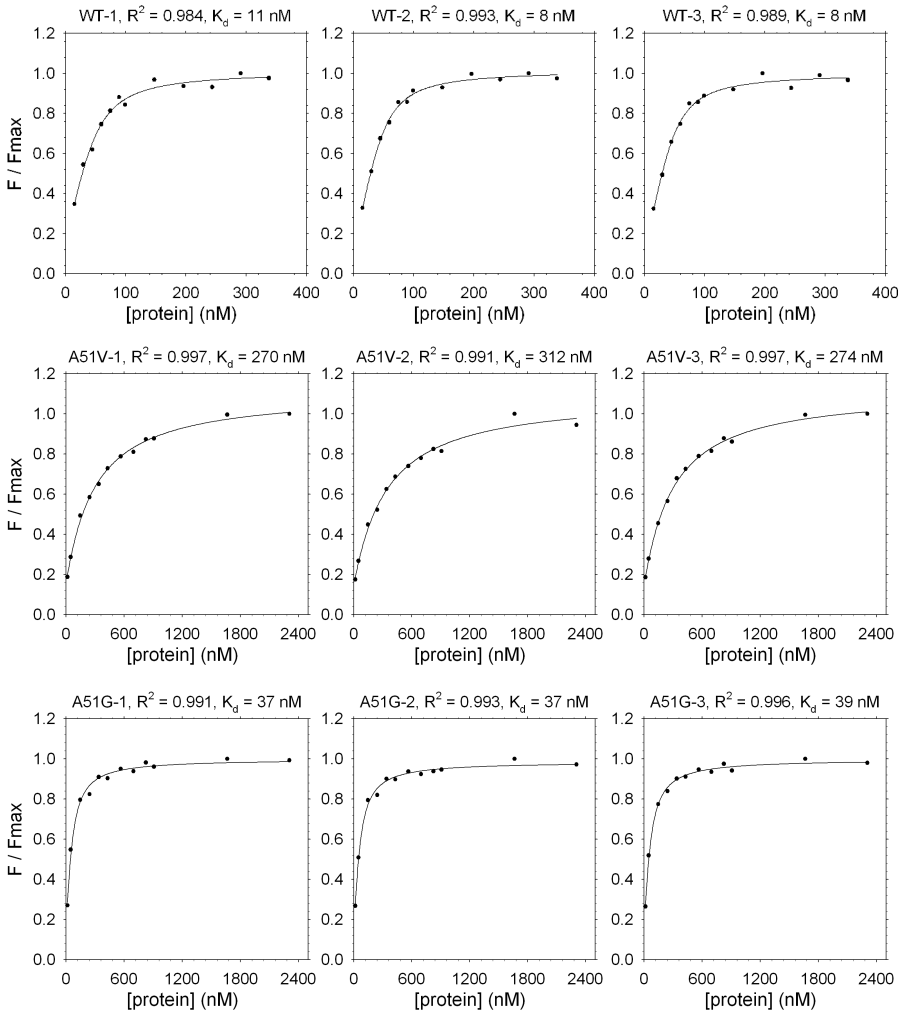

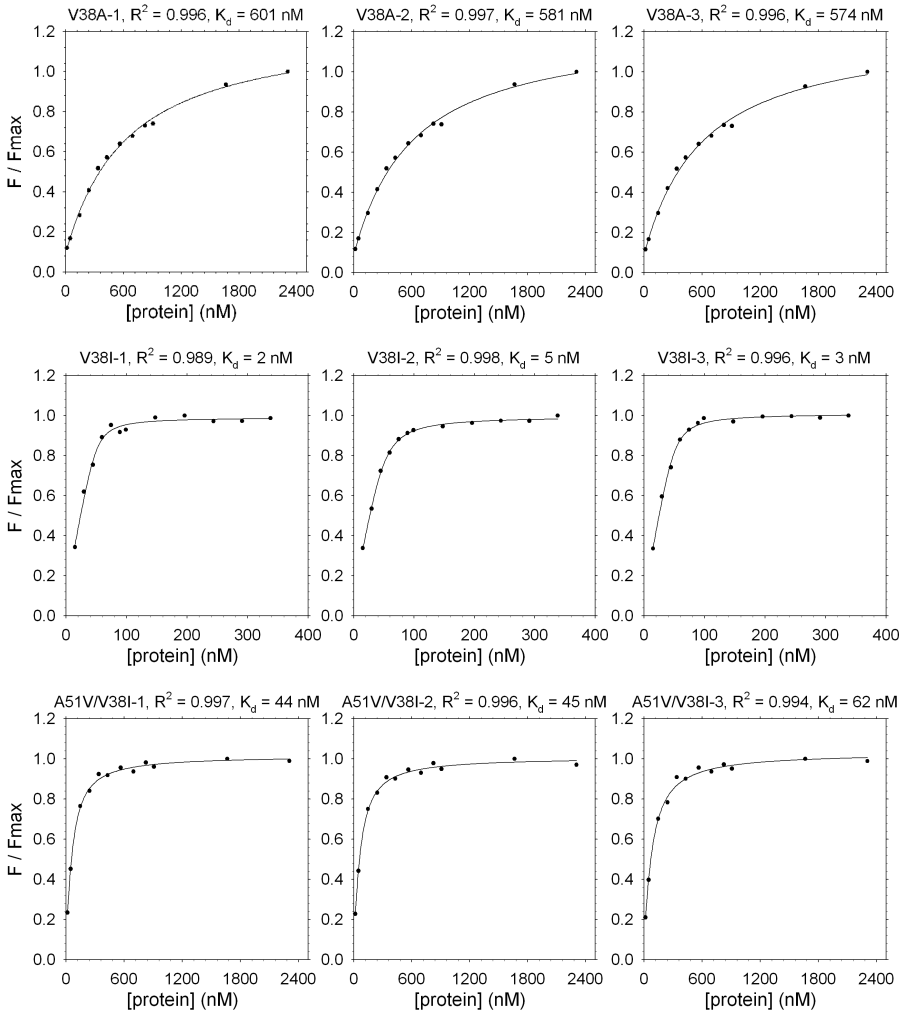
V38A-1, R2 = 0.996, Kd = 601 nM
V38A-2, R2 = 0.997, Kd = 581 nM
V38A-3, R2 = 0.996, Kd = 574 nM
V38I-1, R2 = 0.989, Kd = 2 nM
V38I-2, R2 = 0.998, Kd = 5 nM
V38I-3, R2 = 0.996, Kd = 3 nM
A51V/V38I-1, R2 = 0.997, Kd = 44 nM
A51V/V38I-2, R2 = 0.996, Kd = 45 nM
A51V/V38I-3, R2 = 0.994, Kd = 62 nM
F / Fmax
[protein] (nM)

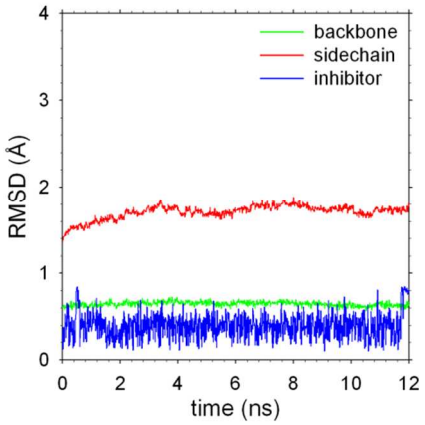

Figure S5. Time dependence of root mean square deviations (RMSDs) for selected groups of atoms in harmonically restrained simulations of wild-type p38α in complex with SB203580. Backbone: the RMSD is calculated for all backbone atoms following alignment of the protein backbone atoms; Sidechain: the RMSD is calculated for all sidechain atoms following alignment of the protein backbone atoms; Inhibitor: the RMSD is calculated for all inhibitor atoms following alignment of the inhibitor atoms. Results are shown for simulations performed with the OPLS-AA/L force field and using a force constant for the position restraints of 0.239 kcal/mol/Å^2.

Figure S6. Plots of $dH/d\lambda$ versus λ for unrestrained and restrained simulations of p38α mutants using the OPLS-AA/L force field. Data from simulations performed without position restraints and with positions restraints using force constants of 0.0239, 0.239, and 2.39 kcal/mol/Å^2 are shown in blue, green, yellow, and red dots, respectively.

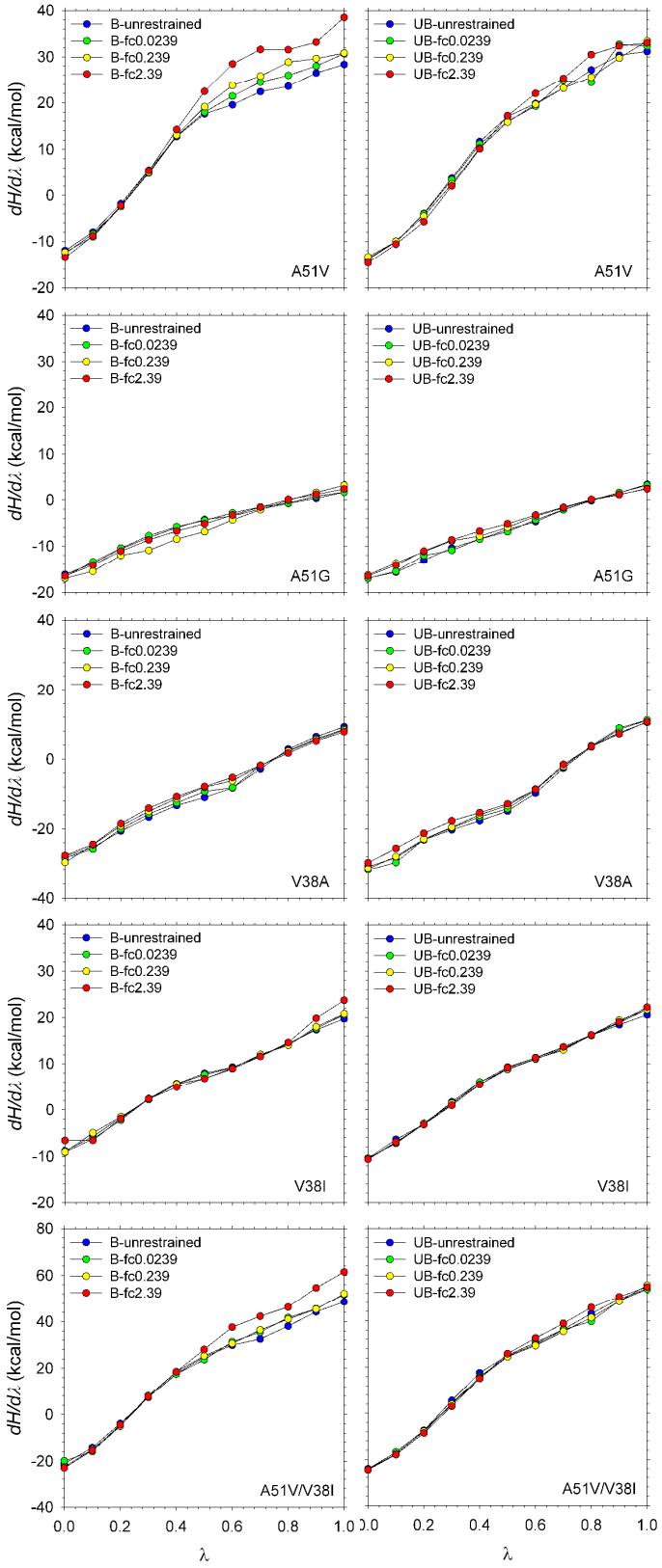
B-unrestrained
B-fc0.0239
B-fc0.239
B-fc2.39
UB-unrestrained
UB-fc0.0239
UB-fc0.239
UB-fc2.39
A51V
A51G
V38A
V38I
A51V/V38I
dH/dλ (kcal/mol)
λ

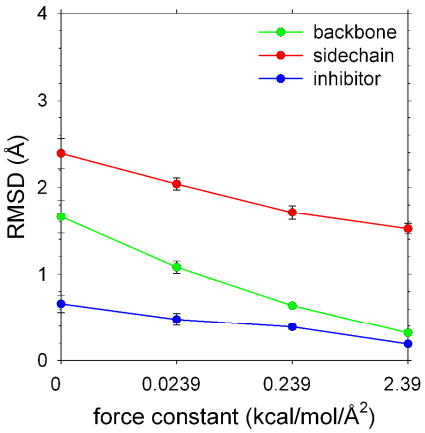

Figure S7. Root mean square deviation (RMSD) versus force constant for 12 ns restrained simulations of wild-type p38α kinase in complex with SB203580 using the OPLS-AA/L force field. Calculations were done for simulations with four sets of force constants: (1) 0 kcal/mol/Å^2 (unrestrained); (2) 0.0239 kcal/mol/Å^2; (3) 0.239 kcal/mol/Å^2; (4) 2.39 kcal/mol/Å^2. Backbone: the RMSD is calculated for all backbone atoms following alignment of the protein backbone atoms; Sidechain: the RMSD is calculated for all sidechain atoms following alignment of the protein backbone atoms; Inhibitor: the RMSD is calculated for all inhibitor atoms following alignment of the inhibitor atoms. Error bars were obtained from block averaging of 1ns simulation blocks.

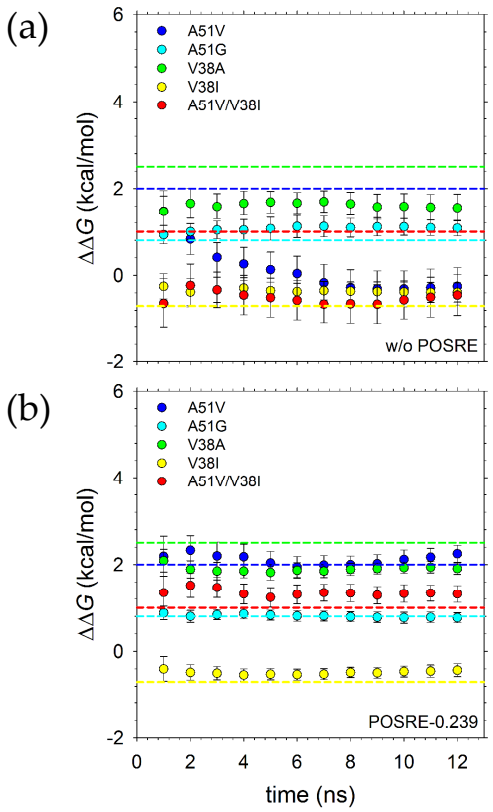

Figure S8. Time dependence of ΔΔG values calculated from simulations using the OPLS-AA/L force field. Results from the unrestrained and restrained (force constant 0.239 kcal/mol/Å^2) simulations are shown in (a) and (b), respectively. The calculated ΔΔG values are shown as solid circles and the corresponding experimental ΔΔG values are shown as horizontal dashed lines of the same color. Each vertical error bar represents the standard deviation of 3[11] independent ΔΔG estimates from three simulation repeats. In all cases, the 'equilibration' phase of the simulations was 0.6 ns.

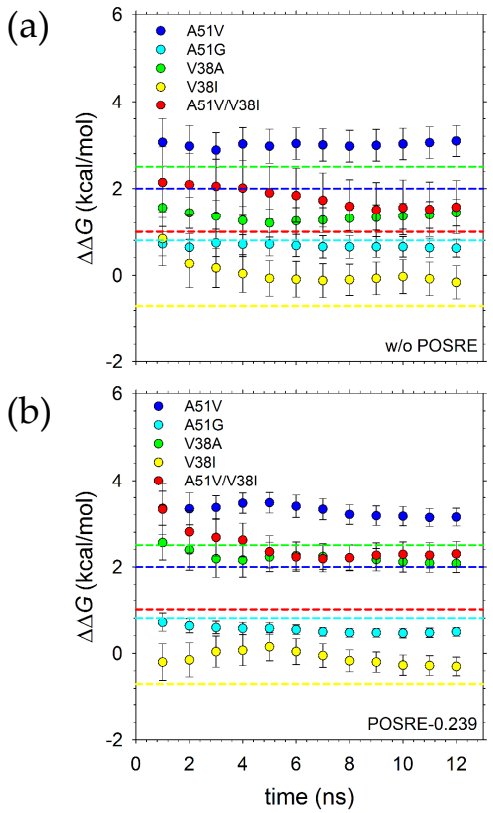

Figure S9. Time dependence of ΔΔG values calculated from simulations using the Amber ff99SB-LDN force field. Results from the unrestrained and restrained (force constant 0.239 kcal/mol/Å^2) simulations are shown in (a) and (b), respectively. The calculated ΔΔG values are shown as solid circles and the corresponding experimental ΔΔG values are shown as horizontal dashed lines of the same color. Each vertical error bar represents the standard deviation of 3[11] independent ΔΔG estimates from three simulation repeats. In all cases, the 'equilibration' phase of the simulations was 0.6 ns.

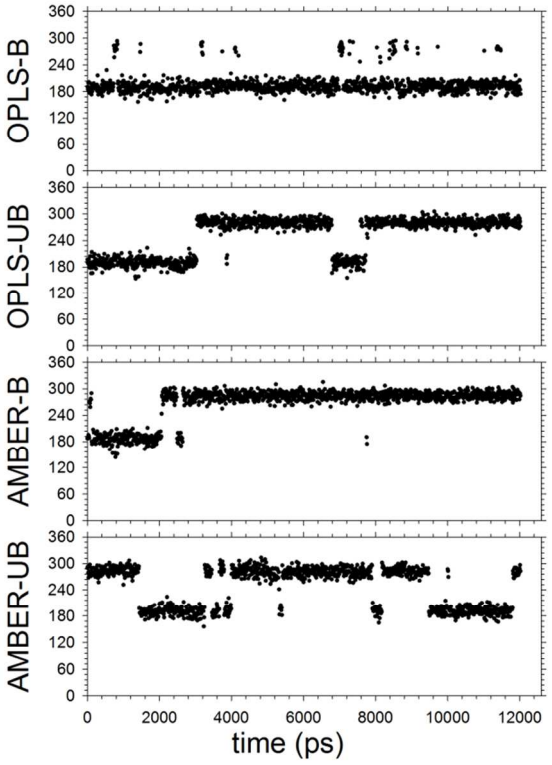

Figure S10. Time dependence of χ1 angles at residue 38 in simulations of the A51V mutant. Angles of 60, 180, 300° correspond to the gauche-, trans, and gauche+ conformation, respectively.

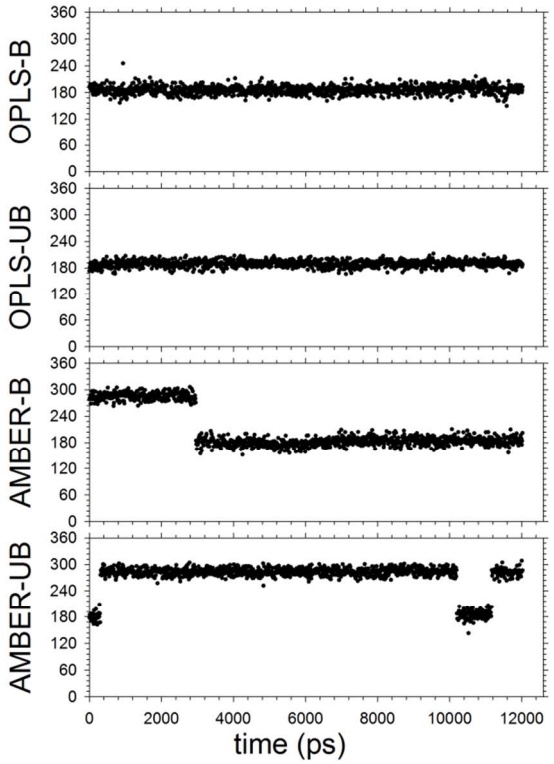

Figure S11. Time dependence of χ1 angles at residue 38 in simulations of the V38I/A51V mutant. Angles of 60, 180, 300° correspond to the gauche-, trans, and gauche+ conformation, respectively.

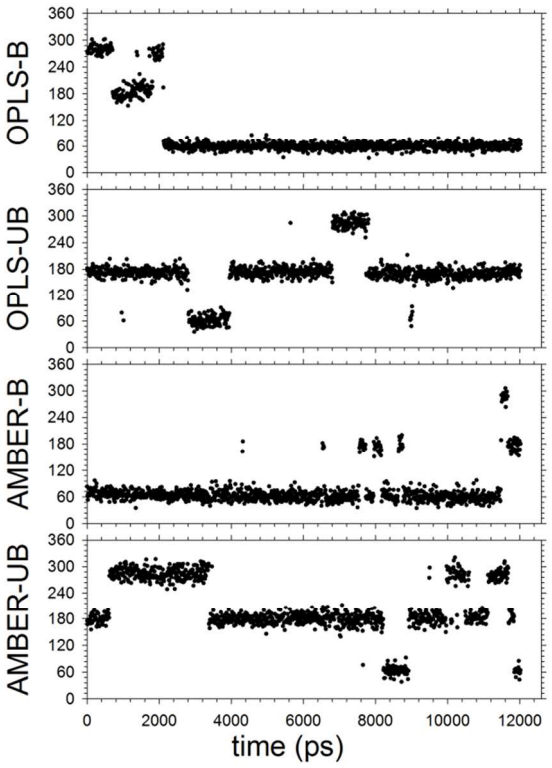

Figure S12. Time dependence of χ1 angles at residue 51 in simulations of the A51V mutant. Angles of 60, 180, 300° correspond to the gauche-, trans, and gauche+ conformation, respectively.

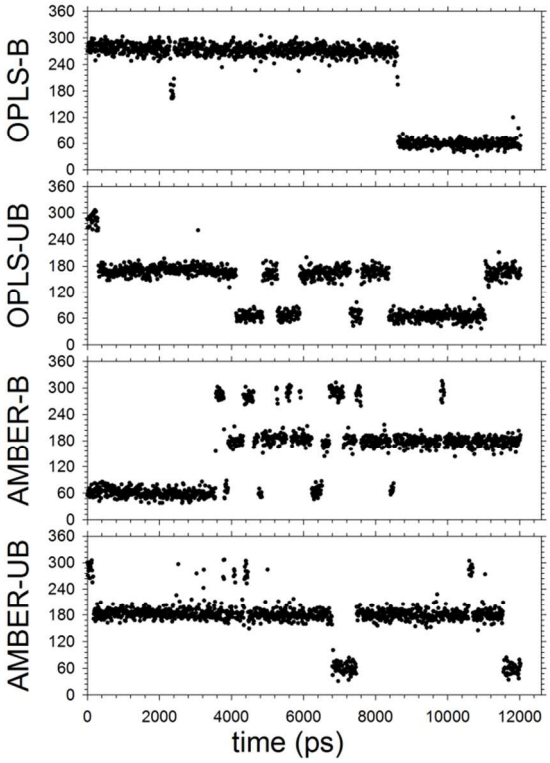

Figure S13. Time dependence of χ1 angles at residue 51 in simulations of the V38I/A51V mutant. Angles of 60, 180, 300° correspond to the gauche-, trans, and gauche+ conformation, respectively.

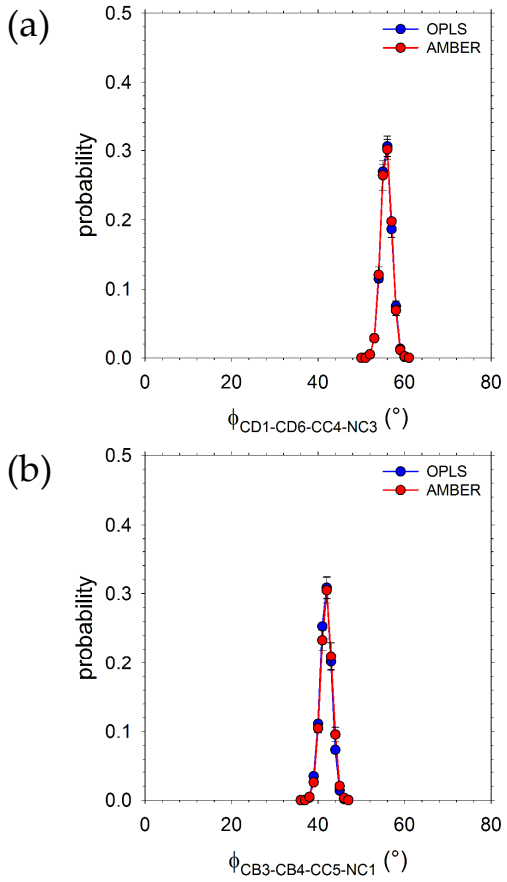

Figure S14. Dihedral angle distributions for inter-ring bonds in the inhibitor in unrestrained simulations in complex with p38a. Two dihedral angles are shown: (a) the dihedral angle that for the bond between the fluorophenyl and imidazole rings, i.e., $\phi_{CD1\text{-}CD6\text{-}CC4\text{-}NC3}$; (b) the dihedral angle for the bond between the pyridine ring and imidazole ring, i.e., $\phi_{CB3\text{-}CB4\text{-}CC5\text{-}NC1}$. The results for OPLS-AA/L and Amber ff99SB-ILDN are shown in blue and red traces, respectively. The error bars were obtained from standard deviation of three 12 ns replicate simulations.

Table S1. Three partial charge sets for the inhibitor SB203580. Partial charges were derived using the CM1A method (CM1A), the analogy method (OPLS-like) and the RESP method (RESP), respectively. The correlation coefficient between pairs of charge sets are: 0.60 (CM1A/OPLS-like), 0.79 (CM1A/RESP), 0.87(OPLS-like/RESP).

Atom name	CM1A	OPLS-like	RESP	Atom name	CM1A	OPLS-like	RESP
CD1	-0.081	-0.115	-0.129	*H11*	0.130	0.060	0.122
HD1	+0.166	0.115	0.138	*H12*	0.139	0.060	0.122
CD2	-0.188	-0.115	-0.227	*H13*	0.146	0.060	0.122
HD2	+0.162	0.115	0.164	*O2*	-0.616	-0.420	-0.474
CD4	-0.186	-0.115	-0.227	*CA4*	-0.069	-0.115	-0.048
HD4	0.162	0.115	0.164	*HA4*	0.146	0.115	0.134
CD5	-0.102	-0.115	-0.129	*CA5*	-0.113	-0.115	-0.179
HD5	0.156	0.115	0.138	*HA5*	0.175	0.115	0.139
CD3	0.076	0.220	0.292	*NC1*	-0.523	-0.291	-0.371
FD3	-0.083	-0.220	-0.204	*HC1*	0.423	0.326	0.327
CD6	-0.026	-0.292	0.028	*CC5*	0.018	-0.196	-0.004
CC4	0.016	0.619	0.178	*CB4*	0.027	0.410	0.114
NC3	-0.275	-0.564	-0.504	*CB3*	-0.198	-0.447	-0.238
CC2	0.161	0.297	0.418	*HB3*	0.154	0.155	0.116
CA6	0.024	-0.017	-0.032	*CB2*	0.003	0.473	0.262
CA1	-0.151	-0.115	-0.179	*HB2*	0.177	0.012	0.076
HA1	0.143	0.115	0.139	*NB1*	-0.308	-0.678	-0.552
CA2	-0.052	-0.115	-0.048	*CB6*	0.003	0.473	0.262
HA2	0.183	0.115	0.134	*HB6*	0.179	0.012	0.076
CA3	-0.349	0.030	0.022	*CB5*	-0.172	-0.447	-0.238
S1	0.818	0.245	0.229	*HB5*	0.174	0.155	0.117
C1	-0.469	-0.035	-0.250				

Table S2. Additional dihedral restraints applied to SB203580 to maintain its "propeller-like" shape. The units for the angle and force constant (fc) are in degrees and kJ/mol/rad^2, respectively.

i	j	k	l	type	label	ϕ	$\Delta\phi$	fc	power
CB5	CB4	CC5	CC4	1	1	42.99	0	4184	2
CB5	CB4	CC5	NC1	1	1	-138.65	0	4184	2
CB3	CB4	CC5	CC4	1	1	-136.12	0	4184	2
CB3	CB4	CC5	NC1	1	1	42.23	0	4184	2
CD1	CD6	CC4	NC3	1	1	56.05	0	4184	2
CD1	CD6	CC4	CC5	1	1	-124.05	0	4184	2
CD5	CD6	CC4	NC3	1	1	-122.52	0	4184	2
CD5	CD6	CC4	CC5	1	1	57.38	0	4184	2